

Heterometallic Pt–Au Complexes with μ -3 S Bridging. Syntheses and Structures of $\text{Pt}_2(\text{PPh}_3)_4(\mu\text{-SAuCl})_2 \cdot 2\text{CH}_2\text{Cl}_2$ and $\text{Pt}_2(\text{PPh}_3)_4(\mu\text{-S})(\mu\text{-SAuPPh}_3)\text{NO}_3 \cdot 0.5\text{H}_2\text{O}$

W. BOS, J. J. BOUR*, P. P. J. SCHLEBOS, P. HAGEMAN, W. P. BOSMAN, J. M. M. SMITS, J. A. C. van WIETMARSCHEN and P. T. BEURSKENS

Department of Inorganic Chemistry and Crystallography, University of Nijmegen, Toernooiveld, 6525 ED Nijmegen, The Netherlands

(Received March 4, 1986)

Abstract

From $\text{Pt}_2(\text{PPh}_3)_4(\mu\text{-S})_2$ (**I**) three heterometallic complexes can be prepared: $\text{Pt}_2(\text{PPh}_3)_4(\mu\text{-SAuCl})_2$ (**II**), $(\text{Pt}_2(\text{PPh}_3)_4(\mu\text{-SAuPPh}_3)_2)^{2+}$ (**III**) and $\text{Pt}_2(\text{PPh}_3)_4(\mu\text{-S})(\mu\text{-SAuPPh}_3)^+$ (**IV**). Their preparation and properties are described.

The crystal and molecular structures of **II** and the nitrate of **IV** has been investigated by X-ray diffraction analysis.

II crystallizes in the monoclinic space group $P2_1/n$, $a = 18.359(2)$, $b = 13.947(2)$, $c = 14.588(2)$ Å, $\beta = 100.982(7)^\circ$, $V = 3666.9$ Å³, $M_r = 2138.28$, $Z = 2$, $D_c = 1.94$ Mg/m³. Mo K α radiation (graphite crystal monochromator, $\lambda = 0.71069$ Å), $\mu(\text{Mo K}\alpha) = 85.13$ cm⁻¹, $F(000) = 2032$, $T = 293$ K. Final conventional R -factor = 0.039, $R_w = 0.050$ for 5084 unique reflections and 155 variables. **IV** crystallizes in the triclinic space group $P\bar{1}$, $a = 14.605(1)$, $b = 15.989(2)$, $c = 18.005(2)$ Å, $\alpha = 101.144(8)^\circ$, $\beta = 100.773(7)^\circ$, $\gamma = 91.201(2)^\circ$, $V = 4045.4$ Å³, $M_r = 2033.75$, $Z = 2$, $D_c = 1.66$ Mg/m³. Cu K α radiation (graphite crystal monochromator, $\lambda = 1.5418$ Å), $\mu(\text{Cu K}\alpha) = 116.45$ cm⁻¹, $F(000) = 1986$, $T = 293$ K. Final conventional R -factor = 0.039 $R_w = 0.051$ for 8631 unique reflections and 297 variables. Both the structures were solved using SHELX84 and DIRDIF.

The hinged square planar geometry of the parent **I** is kept in **IV**, where AuPPh₃ is bonded to one of the bridging S atoms. In **II** both bridging S atoms are bonded to AuCl and the hinging geometry is transformed into a nearly planar P₂PtS₂PtP₂ frame with the SAuCl vectors nearly perpendicular to it, one on each side of that plane. There are indications for weak Au–Pt bonding interactions. In **IV** and **II** the three-coordinated S-atoms have bond angles of about 90°. The structure of **III** is supported to be similar to **II**. Some reactions and interconversions of **II**, **III** and **IV** are described.

* Author to whom correspondence should be addressed.

Introduction

For the preparation of gold clusters we developed procedures using the evaporation of gold and its subsequent reaction in a cold solution of appropriate ligands. As heterometallic complexes and mixed metal clusters have attracted wide attention in recent years and many compounds containing gold in a variety of unusual geometries are known now [1–4], we were engaged in the synthesis of mixed metal clusters by the metal evaporation technique.

The ligating properties of $\text{Fe}_2(\mu\text{-S})_2(\text{CO})_6^{2-}$ and $\text{Pt}_2(\mu\text{-S})_2(\text{PPh}_3)_4$ are well investigated [5, 6], they act as bidentate ligands towards other metal ions to form heterometallic complexes.

Mingos *et al.* [6] described the potential and versatility of $\text{Pt}_2(\mu\text{-S})_2(\text{PPh}_3)_4$ as a bidentate ligand and illustrated this for Pd²⁺ and Hg²⁺ compounds.

Our efforts to prepare mixed Pt–Au clusters by the reaction of gold gas with cold solutions of $\text{Pt}_2(\mu\text{-S})_2(\text{PPh}_3)_4$ were unsuccessful. However, some heterometallic gold platinum complexes were prepared in this way. The properties and structure of three of these compounds were determined and are reported here.

Experimental

Instrumental

C, H and N analyses were carried out in the micro-analytical department of the University of Nijmegen. The other analyses were measured by Dr. A. Bernhardt, Elbach über Engelskirchen, F.R.G. Molecular weights were determined using a Knauer 11.00 vapour pressure osmometer at 37 °C. Electrical conducting measurements were performed with a Metrohm Konduktoskop and a Philips PR 9510/00 conductivity cell at 25 °C.

³¹P [¹H] NMR spectra were recorded on a Varian XL 100 FT at 40.5 MHz, infrared spectra on a Perkin-Elmer 283 spectrophotometer and mass spectra

on a VG 7070 E spectrometer. All materials were of reagent grade.

Preparations

I. $Pt_2(\mu-S)_2(PPh_3)_4$

Prepared as described by Ugo *et al.* [7], from $Pt(PPh_3)_3$ and 2 equivalents of sulfur.

II. $Pt_2(PPh_3)_4(\mu-SAUCl)_2$

Using the rotary metal evaporation apparatus [8], 100 mg Au was evaporated into 200 ml of toluene containing 100 mg of $Pt_2(\mu-S)_2(PPh_3)_4$ and 50 mg of Bu_4NCl at $-100^\circ C$, resulting in a black slurry. After warming up and stirring for 2 h at room temperature a black precipitate is filtered off and the yellow solution is evaporated to about 50 ml. On standing for 24 h yellow crystals are formed. Yield 10% calculated on $Pt_2(\mu-S)_2(PPh_3)_4$. Mass spectrometry: using FAB techniques a parent peak pattern was found around a maximum intensity at 1966 and the isotope ratio was identical with the computer simulation of the formulation $Pt_2(PPh_3)_4(\mu-SAUCl)_2$.

Crystals suitable for X-ray analysis could be obtained by slow diffusion of diethylether into a dichloromethane solution. The crystals are cracked by drying due to loss of CH_2Cl_2 . $Pt_2(PPh_3)_4(\mu-SAUCl)_2$, molecular weight 1968.32. *Anal. Calc.* for $C_{72}H_{60}Au_2Cl_2Pt_2S_2P_4$: Au, 20.02; Pt, 19.81; S, 3.25. Found: Au, 19.70; Pt, 19.85; S, 3.07%. The IR spectrum is the same as that of $Pt_2(\mu-S)_2(PPh_3)_4$ except for a weak Au-Cl stretching band at 330 cm^{-1} , $^{31}P[^1H]$ NMR in CH_2Cl_2 relative to TMP 18.88 ppm $^1J(PtP)$ 3030 Hz.

III. $Pt_2(PPh_3)_4(\mu-SAUPh_3)_2(NO_3)_2$

To a suspension of 100 mg of $Pt_2(\mu-S)_2(PPh_3)_4$ in 35 ml THF a solution of 68 mg of $AuPPh_3NO_3$ (molar ratio 1:2) in 5 ml THF is added under stirring.

When nearly 1 equivalent is added the solution becomes clear yellow and by adding more a beige product precipitates. The product is filtered off and washed with THF and diethylether and dried under vacuo (yield 150 mg, 90%). $Pt_2(PPh_3)_4(\mu-SAUPh_3)_2(NO_3)_2$; molecular weight 2546.01. *Anal. Calc.* for $C_{108}H_{90}Au_2Pt_2N_2O_6P_6S_2$: C, 50.95; H, 3.54; N, 1.10; Au, 15.47; Pt, 15.33; S, 2.52. Found C, 49.51; H, 3.41; N, 0.99; Au, 15.55; Pt, 15.30; S, 2.49%. Conductivity $59.2\text{ ohm}^{-1}\text{ cm}^2\text{ mol}^{-1}$ in DMSO at $25^\circ C$; molecular weight determination 3000; $^{31}P[^1H]$ NMR in CH_2Cl_2 relative to TMP 18.80 ppm, (4P, $PtPPh_3$) $^1J(PtP)$ 2900 Hz, 32.90 ppm (2P, $AuPPh_3$).

IV. $Pt_2(PPh_3)_4(\mu-S)(\mu-SAUPh_3)NO_3 \cdot 0.5H_2O$

(a) When a solution of 17.5 mg of $AuPPh_3NO_3$ (0.03 mmol) in 2 ml of THF is added to a suspension

of 50 mg of $Pt_2(\mu-S)_2(PPh_3)_4$ (0.03 mmol) in 8 ml of THF, a clear yellow solution is formed within 15 min and after 24 h yellow crystals are formed. The crystals suitable for an X-ray analysis are filtered off, washed with 2 ml of THF and diethylether and dried *in vacuo*. Yield 18 mg, 25% $Pt_2(PPh_3)_4(\mu-S)(\mu-SAUPh_3)NO_3 \cdot \frac{1}{2}H_2O$, molecular weight 2033.75. *Anal. calc.* for $C_{90}H_{75}AuPt_2NO_3P_5S_2 \cdot \frac{1}{2}H_2O$: C, 53.31; H, 3.77; N, 0.69; Pt, 19.18; Au, 9.69; P, 7.61; S, 3.15. Found: C, 53.16; H, 3.83; N, 0.71; Pt, 19.20; Au, 9.88; P, 7.55; S, 3.06%.

Conductivity $49.5\text{ ohm}^{-1}\text{ cm}^2\text{ mol}^{-1}$ in DMSO at $25^\circ C$, $^{31}P[^1H]$ NMR in CH_2Cl_2 relative to TMP, 17.95 ppm (4P, $PtPPh_3$), $^1J(PtP)$ 2990 Hz, 29.22 ppm (P, $AuPPh_3$).

In a similar procedure but using $AuPPh_3Cl$ instead of $AuPPh_3NO_3Pt_2(PPh_3)_4(\mu-S)(\mu-SAUPh_3)Cl$ was obtained. Excess of $AuPPh_3Cl$ does not yield any other product.

(b) When 50 mg of metallic gold is evaporated in 100 ml toluene containing 100 mg $Pt_2(\mu-S)(PPh_3)_4$ and 50 mg PPh_3 a black brown slurry is formed. To this slurry 100 ml dichloromethane is added and after one hour the dark solid is filtered off and the brown solution is concentrated by evaporation to 50 ml. After one day a red-brown precipitate is formed. The precipitate is filtered off and washed with 50 ml of THF. The $^{31}P[^1H]$ NMR spectrum of the soluble part of the precipitate in CH_2Cl_2 shows $Pt_2(PPh_3)_4(\mu-S)(\mu-SAUPh_3)^+$ as the main product.

Crystal Structure Determination

II. $Pt_2(PPh_3)_4(\mu-SAUCl)_2 \cdot 2CH_2Cl_2$ and IV. $Pt_2(PPh_3)_4(\mu-S)(\mu-SAUPh_3)NO_3 \cdot 0.5H_2O$

Suitable yellow crystals of **II** and **IV** were used for the measurements. To prevent cracking by loss of CH_2Cl_2 the crystal of **II** was mounted in a glass capillary with solvent throughout the experiment. Mo $K\alpha$ radiation (**II**) ($\lambda = 0.71069\text{ \AA}$) and Cu $K\alpha$ radiation (**IV**) ($\lambda = 1.5418\text{ \AA}$) were used at 293 K with a graphite crystal monochromator on a Nonius CAD4 single crystal diffractometer. The unit cell dimensions, **II**: monoclinic, $a = 18.359(2)$, $b = 13.947(2)$, $c = 14.588(2)\text{ \AA}$, $\beta = 100.982(7)^\circ$, $V = 3666.9\text{ \AA}^3$, **IV**: triclinic, $a = 14.605(1)$, $b = 15.989(2)$, $c = 18.005(2)\text{ \AA}$, $\alpha = 101.144(8)^\circ$, $\beta = 100.773(7)^\circ$, $\gamma = 91.201(2)^\circ$, $V = 4045.4\text{ \AA}^3$, were determined from the angular settings of 22 reflections with $14^\circ < \theta < 28^\circ$ for **II** and of 25 reflections with $15^\circ < \theta < 57^\circ$ for **IV**. The space groups were determined from the systematic absences and the structure determination. **II**: $P2_1/n$; $h0l$, $h + l = 2n + 1$; $0k0$, $k = 2n + 2$; **IV**: $P\bar{1}$. The intensity data of 6845 (**II**) (to $\theta = 25^\circ$) and 14419 reflections (**IV**) (to $\theta = 55^\circ$) were measured using the ω - 2θ scan technique, with a scan angle of 1.00° and a variable

scan rate with a maximum scan time of 20 s per reflection.

The intensity of the primary beam was checked throughout the data collection by monitoring three reference reflections every 30 min. The final drift correction factors were between 0.95 and 1.03 (II) and 0.96 and 1.04 (IV). A smooth curve based on the reference reflections was used to correct for this drift. On all reflections profile analysis was performed [9, 10]; empirical absorption correction was applied using ψ scans [11]. For II: $\mu(Mo K\alpha) = 85.13 \text{ cm}^{-1}$ (correction factors were in the range 0.70 to 1.00; for IV: $\mu(Cu K\alpha) = 116.5 \text{ cm}^{-1}$ (correction factors were in the range 0.68 to 1.00); Symmetry equivalent reflections were averaged, $R_{int} = \Sigma(I - \langle I \rangle) / \Sigma I = 0.029$ (II) and 0.018 (IV) resulting in 6845 (II) and 10144 (IV) unique reflections of which 5084 (II) and 8631 (IV) were observed with $I > 3\sigma(I)$. Lorentz and polarization corrections were applied and the data were reduced to $|F_o|$ -values.

The gold and platinum atoms were found using SHELX84 [12]. The structures were expanded using DIRDIF [13], thereby establishing the chemical composition. The structures were refined by full-matrix least-squares on $|F|$ values, using SHELX [14]. Scattering factors were taken from International Tables [15]. Two dichloromethane molecules (II) and a half of water molecule (IV) were found from the respectively difference Fourier syntheses and were included in the refinement. Hydrogen atoms were found from difference Fourier syntheses and were included in the refinement. The phenyl type carbon atoms were converted into a regular hexagon with carbon-carbon distances

1.395 Å and all hydrogen atoms were included in fixed idealized positions 1.08 Å from the carbon atom to which they were bonded. Isotropic refinement converged to $R = 0.085$ (II) and 0.063 (IV). At this stage empirical absorption correction was applied [16], resulting in a further decrease of R to 0.072 (II) (correction factors were in the range 0.87–1.13) and to 0.054 (IV) (correction factors were in the range 0.88–1.30). No extinction corrections were applied.

During the final stages of the refinement the positional parameters of the non-phenyl atoms, the anisotropic thermal parameters of gold, platinum, phosphorus, sulfur and chlorine (II) and the isotropic thermal parameters of the carbon atoms were refined. The phenyl groups were refined as rigid groups with standard geometry. The hydrogen atoms had fixed isotropic temperature factors of 0.05 Å. The final conventional agreement factors were for II: $R = 0.039$ and $R_w = 0.050$ for the 5084 'observed' reflections and 155 variables, for IV: $R = 0.039$ and $R_w = 0.051$ for the 8631 'observed' reflections and 297 variables. The function minimized was $\Sigma w(F_o - F_c)^2$ with $w = \sigma(F_o + 0.0004 F_c)^{-2}$ with $\sigma(F_o)$ from counting statistics. The maximum shift over error ratio in the last full matrix least-squares cycle was for II less than 0.20 except for dichloromethane (up to 1.46) and for IV less than 0.22. The final difference Fourier map showed for II one peak of height 3 $e/\text{Å}^3$ at 0.9 Å from Au and several peaks of about 1 $e/\text{Å}^3$; and for IV no peaks higher than 0.5 $e/\text{Å}^3$. Plots were made with PLUTO [17]. Final positional and thermal parameters are given in Table I. Molecular geometry data are collected in Tables

TABLE I. Fractional Positional and Thermal Parameters (e.s.d. Values in Parentheses): (a) $Pt_2(PPh_3)_4(\mu-SAUCI)_2 \cdot 2CH_2Cl_2$. (b) $Pt_2(PPh_3)_4(\mu-SAUPPh_3)(\mu-S)(NO_3)_2 \cdot 0.5H_2O$

Atom	x	y	z	U_{eq} ($\times 100$) (Å^2)
(a)				
Au1	0.11371(2)	0.03719(3)	0.13273(3)	4.59(1)
Pt1	-0.05595(2)	-0.00375(2)	0.08737(2)	2.22(1)
S1	0.04795(11)	-0.08342(14)	0.04903(14)	3.12(6)
P1	-0.05986(11)	-0.12011(14)	0.19668(14)	2.81(6)
P2	-0.14327(11)	0.09878(14)	0.12111(14)	2.68(6)
Cl1	0.1683(2)	0.1645(3)	0.2185(3)	10.3(2)
C1	0.0323(3)	-0.1514(3)	0.2612(4)	3.5(2)
C2	0.0764(3)	-0.0781(3)	0.3074(4)	4.2(2)
C3	0.1485(3)	-0.0979(3)	0.3540(4)	5.4(3)
C4	0.1764(3)	-0.1909(3)	0.3544(4)	6.1(3)
C5	0.1323(3)	-0.2642(3)	0.3083(4)	6.1(3)
C6	0.0602(3)	-0.2445(3)	0.2617(4)	4.6(2)
C7	-0.0950(3)	-0.2308(4)	0.1396(3)	3.6(2)
C8	-0.1121(3)	-0.3072(4)	0.1935(3)	4.8(2)
C9	-0.1381(3)	-0.3933(4)	0.1507(3)	6.6(3)
C10	-0.1471(3)	-0.4029(4)	0.0540(3)	6.8(3)
C11	-0.1300(3)	-0.3265(4)	0.0001(3)	5.9(3)

(continued)

TABLE I. (continued)

Atom	x	y	z	U_{eq} ($\times 100$) (\AA^2)
C12	-0.1040(3)	-0.2404(4)	0.0429(3)	4.1(2)
C13	-0.1170(2)	-0.1078(5)	0.2861(4)	3.4(2)
C14	-0.0861(2)	-0.0835(5)	0.3780(4)	4.6(2)
C15	-0.1312(2)	-0.0757(5)	0.4445(4)	6.2(3)
C16	-0.2074(2)	-0.0923(5)	0.4190(4)	5.4(3)
C17	-0.2383(2)	-0.1166(5)	0.3271(4)	5.7(3)
C18	-0.1931(2)	-0.1244(5)	0.2606(4)	4.4(2)
C19	-0.2398(3)	0.0596(4)	0.0885(4)	3.5(2)
C20	-0.2533(3)	-0.0307(4)	0.0477(4)	4.9(2)
C21	-0.3261(3)	-0.0632(4)	0.0199(4)	6.6(3)
C22	-0.3853(3)	-0.0054(4)	0.0329(4)	7.0(3)
C23	-0.3717(3)	0.0850(4)	0.0737(4)	7.0(3)
C24	-0.2990(3)	0.1174(4)	0.1015(4)	5.0(2)
C25	-0.1421(3)	0.2110(4)	0.0575(4)	3.2(2)
C26	-0.1883(3)	0.2203(4)	-0.0298(4)	4.3(2)
C27	-0.1803(3)	0.2988(4)	-0.0865(4)	6.2(3)
C28	-0.1262(3)	0.3679(4)	-0.0558(4)	6.3(3)
C29	-0.0801(3)	0.3585(4)	0.0315(4)	6.4(3)
C30	-0.0880(3)	0.2801(4)	0.0881(4)	5.0(2)
C31	-0.1233(2)	0.1332(4)	0.2445(4)	3.1(2)
C32	-0.1778(2)	0.1445(4)	0.2984(4)	4.2(2)
C33	-0.1583(2)	0.1743(4)	0.3911(4)	5.4(3)
C34	-0.0842(2)	0.1929(4)	0.4300(4)	6.0(3)
C35	-0.0296(2)	0.1817(4)	0.3761(4)	5.9(3)
C36	-0.0492(2)	0.1519(4)	0.2834(4)	4.2(2)
C12	0.3132(3)	-0.0480(4)	0.2262(4)	12.9(2)
C13	0.4700(3)	0.9581(5)	0.2323(5)	18.1(3)
C37	0.391(1)	0.891(2)	0.206(1)	13.4(7)
(b)				
Pt1	0.21128(2)	0.21003(2)	0.32619(2)	2.265(12)
Pt2	0.23208(2)	0.26916(2)	0.16532(2)	1.974(12)
Au1	0.02550(3)	0.24158(2)	0.19991(2)	3.571(14)
S1	0.15119(14)	0.15336(11)	0.19334(10)	2.45(6)
S2	0.20075(15)	0.33911(11)	0.28426(11)	2.64(7)
P1	0.25742(17)	0.27872(13)	0.45070(12)	3.23(8)
P2	0.22231(17)	0.07144(13)	0.34259(12)	3.23(8)
P3	0.25272(15)	0.19121(12)	0.05006(11)	2.57(7)
P4	0.30829(15)	0.39438(12)	0.16123(11)	2.46(7)
P5	-0.11216(17)	0.30180(15)	0.19612(14)	3.81(9)
N1	0.5561(9)	0.7252(7)	0.2111(7)	8.8(3)
O1	0.5551(8)	0.7736(7)	0.1647(7)	13.4(4)
O2	0.4807(8)	0.6811(7)	0.1987(6)	11.9(3)
O3	0.6262(8)	0.7058(7)	0.2530(6)	12.4(4)
O4	0.6987(11)	0.8968(9)	0.2330(8)	6.8(4)
C1A	0.2088(3)	0.2234(4)	0.5812(3)	4.8(3)
C2A	0.1432(3)	0.1960(4)	0.6199(3)	6.7(3)
C3A	0.0484(3)	0.1892(4)	0.5864(3)	6.8(3)
C4A	0.0193(3)	0.2099(4)	0.5142(3)	7.0(3)
C5A	0.0849(3)	0.2373(4)	0.4755(3)	5.6(3)
C6A	0.1796(3)	0.2440(4)	0.5089(3)	3.8(2)
C7A	0.4354(4)	0.2232(4)	0.4473(3)	4.9(3)
C8A	0.5288(4)	0.2138(4)	0.4780(3)	6.4(3)
C9A	0.5656(4)	0.2492(4)	0.5552(3)	7.2(3)
C10A	0.5092(4)	0.2941(4)	0.6018(3)	6.6(3)

(continued)

TABLE I. (continued)

Atom	x	y	z	$Y_{eq}(\times 100) (\text{\AA}^2)$
C11A	0.4159(4)	0.3035(4)	0.5711(3)	5.5(3)
C12A	0.3790(4)	0.2681(4)	0.4938(3)	3.7(2)
C13A	0.3230(4)	0.4413(4)	0.4479(4)	5.5(3)
C14A	0.3206(4)	0.5298(4)	0.4569(4)	7.1(3)
C15A	0.2485(4)	0.5718(4)	0.4866(4)	7.4(3)
C16A	0.1789(4)	0.5252(4)	0.5073(4)	7.1(3)
C17A	0.1813(4)	0.4367(4)	0.4984(4)	5.8(3)
C18A	0.2533(4)	0.3948(4)	0.4687(4)	3.9(2)
C1B	0.3431(5)	-0.0613(4)	0.3148(4)	6.3(3)
C2B	0.4149(5)	-0.1004(4)	0.2824(4)	7.8(4)
C3B	0.4628(5)	-0.0583(4)	0.2390(4)	8.0(4)
C4B	0.4390(5)	0.0231(4)	0.2279(4)	6.0(3)
C5B	0.3672(5)	0.0623(4)	0.2603(4)	3.9(2)
C6B	0.3192(5)	0.0201(4)	0.3037(4)	3.9(2)
C7B	0.1188(4)	-0.0743(4)	0.2474(4)	6.5(3)
C8B	0.0360(4)	-0.1236(4)	0.2146(4)	8.9(4)
C9B	-0.0493(4)	-0.0917(4)	0.2266(4)	8.0(4)
C10B	-0.0519(4)	-0.0105(4)	0.2714(4)	7.3(3)
C11B	0.0309(4)	0.0388(4)	0.3041(4)	5.9(3)
C12B	0.1163(4)	0.0069(4)	0.2921(4)	3.9(2)
C13B	0.3289(4)	0.0500(4)	0.4820(4)	6.4(3)
C14B	0.3437(4)	0.0316(4)	0.5558(4)	10.3(5)
C15B	0.2686(4)	0.0044(4)	0.5848(4)	10.4(5)
C16B	0.1788(4)	-0.0045(4)	0.5399(4)	9.1(4)
C17B	0.1640(4)	0.0139(4)	0.4661(4)	6.3(3)
C18B	0.2391(4)	0.0412(4)	0.4371(4)	4.5(2)
C1C	0.3949(4)	0.1191(4)	-0.0228(2)	4.5(2)
C2C	0.4867(4)	0.0975(4)	-0.0236(2)	5.9(3)
C3C	0.5558(4)	0.1237(4)	0.0423(2)	5.9(3)
C4C	0.5331(4)	0.1716(4)	0.1091(2)	5.4(3)
C5C	0.4412(4)	0.1933(4)	0.1099(2)	3.7(2)
C6C	0.3721(4)	0.1670(4)	0.0440(2)	3.0(2)
C7C	0.2469(3)	0.2495(3)	-0.0903(3)	3.1(2)
C8C	0.2036(3)	0.2900(3)	-0.1484(3)	4.1(2)
C9C	0.1174(4)	0.3247(3)	-0.1446(3)	4.5(2)
C10C	0.0744(3)	0.3188(3)	-0.0827(3)	4.6(2)
C11C	0.1176(3)	0.2783(3)	-0.0246(3)	3.7(2)
C12C	0.2038(3)	0.2436(3)	-0.0284(3)	2.6(2)
C13C	0.1163(4)	0.0639(3)	-0.0369(3)	4.7(2)
C14C	0.0758(4)	-0.0192(3)	-0.0574(3)	6.5(3)
C15C	0.1152(4)	-0.0825(3)	-0.0203(3)	6.4(3)
C16C	0.1951(4)	-0.0628(3)	0.0374(3)	5.9(3)
C17C	0.2357(4)	0.0203(3)	0.0579(3)	4.5(2)
C18C	0.1963(4)	0.0836(3)	0.0207(3)	3.0(2)
C1D	0.1427(4)	0.4741(3)	0.1681(3)	3.9(2)
C2D	0.0874(4)	0.5422(3)	0.1864(3)	5.3(3)
C3D	0.1291(4)	0.6215(3)	0.2265(3)	6.2(3)
C4D	0.2261(4)	0.6325(3)	0.2483(3)	7.1(3)
C5D	0.2814(4)	0.5644(3)	0.2300(3)	6.0(3)
C6D	0.2397(4)	0.4851(3)	0.1900(3)	2.9(2)
C7d	0.4436(4)	0.3708(3)	0.2865(3)	3.7(2)
C8D	0.5279(4)	0.3904(3)	0.3393(3)	5.1(3)
C9D	0.5895(4)	0.4552(3)	0.3329(3)	5.9(3)
C10D	0.5670(4)	0.5005(3)	0.2737(3)	4.8(3)
C11D	0.4828(4)	0.4810(3)	0.2209(3)	3.8(2)
C12D	0.4211(4)	0.4162(3)	0.2274(3)	2.4(2)
C13D	0.2770(3)	0.4612(3)	0.0267(3)	3.7(2)
C14D	0.1975(3)	0.4764(3)	-0.0423(3)	4.9(3)

(continued)

TABLE I. (continued)

Atom	x	y	z	$U_{eq}(\times 100)(\text{\AA}^2)$
C15D	0.3777(3)	0.4453(3)	-0.0668(3)	4.9(3)
C16D	0.4374(3)	0.3990(3)	-0.0223(3)	4.9(3)
C17D	0.4169(3)	0.3838(3)	0.0467(3)	3.7(2)
C18D	0.3367(3)	0.4149(3)	0.0713(3)	2.8(2)
C1E	-0.1248(3)	0.3263(4)	0.0464(4)	6.0(3)
C2E	-0.1706(3)	0.3282(4)	-0.0285(4)	7.5(3)
C3E	-0.2667(3)	0.3093(4)	-0.0502(4)	6.6(3)
C4E	-0.3170(3)	0.2884(4)	0.0030(4)	6.3(3)
C5E	-0.2712(3)	0.2865(4)	0.0779(4)	5.5(3)
C6E	-0.1752(3)	0.3055(4)	0.0996(4)	3.7(2)
C7E	-0.2100(5)	0.1555(4)	0.2051(3)	6.2(3)
C8E	-0.2709(5)	0.1075(4)	0.2339(3)	7.0(3)
C9E	-0.3138(5)	0.1466(4)	0.2936(3)	8.1(4)
C10E	-0.2959(5)	0.2337(4)	0.3244(3)	8.3(4)
C11E	-0.2350(5)	0.2816(4)	0.2956(3)	6.5(3)
C12E	-0.1920(5)	0.2426(4)	0.2359(3)	4.4(2)
C13E	-0.0259(4)	0.4419(4)	0.3034(4)	5.7(3)
C14E	-0.0190(4)	0.5258(4)	0.3450(4)	6.9(3)
C15E	-0.0932(4)	0.5783(4)	0.3328(4)	6.1(3)
C16E	-0.1741(4)	0.5470(4)	0.2791(4)	5.5(3)
C17E	-0.1810(4)	0.4631(4)	0.2375(4)	5.3(3)
C18E	-0.1069(4)	0.4106(4)	0.2497(4)	4.2(2)

TABLE II. Atomic Distances (e.s.d. Values in Parentheses): (a) $\text{Pt}_2(\text{PPh}_3)_4(\mu\text{-SAuCl})_2 \cdot 2\text{CH}_2\text{Cl}_2$. (b) $\text{Pt}_2(\text{PPh}_3)_4(\mu\text{-SAu-PPh}_3)(\mu\text{-S})(\text{NO}_3)_2 \cdot 0.5\text{H}_2\text{O}$

(a)			
Au1-Pt1	3.111(1)	Pt1-P1	2.286(2)
Au1-Pt1'	3.218(1)	Pt1-P2	2.271(2)
Au1-S1	2.284(2)		
Au1-Cl1	2.290(3)		
Pt1-S1	2.365(2)		
Pt1-S1'	2.360(2)		
(b)			
Pt1-Pt2	3.279(1)	Au1-S1	2.345(2)
Pt1-Au1	3.314(1)	Au1-S2	2.959(2)
Pt1-S1	2.378(2)	Au1-P5	2.243(2)
Pt1-S2	2.329(2)		
Pt1-P1	2.267(2)		
Pt1-P2	2.296(2)		
Pt2-Au1	3.231(1)		
Pt2-S1	2.360(2)		
Pt2-S2	2.347(2)		
Pt2-P3	2.280(2)		
Pt2-P4	2.291(2)		

II and III. The molecular configuration and the crystallographic numbering scheme is given in Fig. 1a and b. No unusual intermolecular contacts are present in both the structures.

Results and Discussion

The $\text{Pt}_2(\text{PPh}_3)_4(\mu\text{-SAuCl})_2$ complex is formed when metallic gold is evaporated into a toluene solution containing Bu_4NCl and $\text{Pt}_2(\mu\text{-S})_2(\text{PPh}_3)_4$. That $\text{Pt}_2(\text{PPh}_3)_4(\mu\text{-SAuCl})_2$ is formed in the metal evaporation apparatus and not during the recrystallization in CH_2Cl_2 can be concluded from mass spectral data of the products precipitated from the toluene solution. Using FAB techniques a parent peak pattern was found around a maximum intensity at 1966, and the isotope ratio was identical with the computer simulation of the formulation $\text{Pt}_2(\text{PPh}_3)_4(\mu\text{-SAuCl})_2$. The reaction path in the metal evaporation experiment is unknown. The oxidation of the gold to Au(I) may be due to traces of air or water in the apparatus [8, 19]. Interestingly we found that neither AuCl nor $\text{Au}(\text{CO})\text{Cl}$ reacts with $\text{Pt}_2(\text{PPh}_3)_4\text{S}_2$ to form $\text{Pt}_2(\text{PPh}_3)_4(\mu\text{-AuCl})_2$. The Au-Pt compounds described in this paper are in general inert to CH_2Cl_2 , which is noteworthy as the parent $\text{Pt}_2(\text{PPh}_3)_4\text{S}_2$ reacts with CH_2Cl_2 to form the S-methylated $\text{Pt}_2(\text{PPh}_3)_4(\mu\text{-S})(\mu\text{-SCH}_2\text{Cl})^+$ [18].

The crystal structure determination shows $\text{Pt}_2(\text{PPh}_3)_4(\mu\text{-SAuCl})_2$ to have in good approximation C_{2h} symmetry with the Pt-Pt vector as the local two-fold axis. The hinged squares present in the parent compound $\text{Pt}_2(\text{PPh}_3)_4\text{S}_2$ are bent to a flat structure

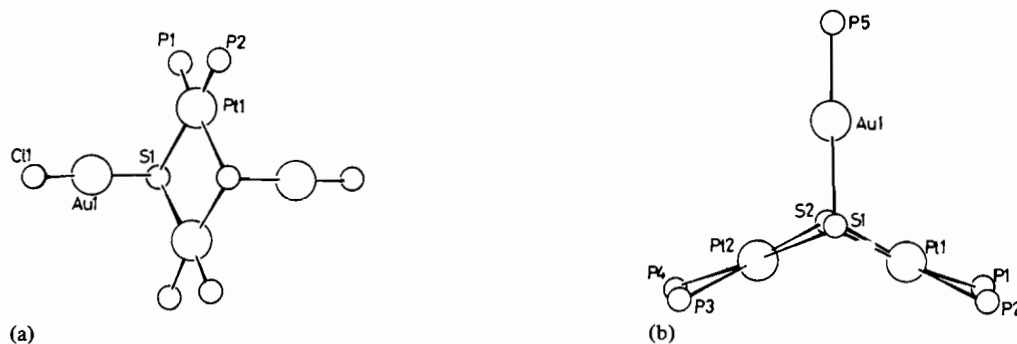


Fig. 1. Molecular configuration and atomic numbering scheme for (a) $\text{Pt}_2(\text{PPh}_3)_4(\mu\text{-SAuCl})_2 \cdot 2\text{CH}_2\text{Cl}_2$; (b) $\text{Pt}_2(\text{PPh}_3)_4(\mu\text{-S})(\mu\text{-AuPPh}_3)(\text{NO}_3)_2 \cdot 0.5\text{H}_2\text{O}$.

TABLE III. Bond Angles (e.s.d. Values in Parentheses); (a) $\text{Pt}_2(\text{PPh}_3)_4(\mu\text{-SAuCl})_2 \cdot 2\text{CH}_2\text{Cl}_2$. (b) $\text{Pt}_2(\text{PPh}_3)_4(\mu\text{-SAuPPh}_3)(\mu\text{-S})(\text{NO}_3)_2 \cdot 0.5\text{H}_2\text{O}$

(a)			
Pt1–Au1–Pt1'	68.6(1)	Au1'–Pt1–P1	123.0(1)
Pt1–Au1–S1	49.1(1)	Au1'–Pt1–P2	101.3(1)
Pt1'–Au1–S1	47.1(1)	S1–Pt1–S1'	82.0(1)
Pt1–Au1–Cl1	125.1(1)	S1–Pt1–P1	88.0(1)
Pt1'–Au1–Cl1	133.2(1)	S1–Pt1–P2	169.0(2)
S1–Au1–Cl1	174.2(1)	S1'–Pt1–P1	165.7(1)
Au1–Pt1–Au1'	111.4(1)	S1'–Pt1–P2	91.0(1)
Au1–Pt1–S1	46.9(1)	P1–Pt1–P2	100.3(1)
Au1–Pt1–S1'	82.0(1)	Au1–S1–Pt1	84.0(1)
Au1'–Pt1–S1	79.8(1)	Au1–S1–Pt1'	87.7(1)
Au1'–Pt1–S1'	45.2(1)	Pt1–S1–Pt1	98.0(1)
Au1–Pt1–P1	98.3(1)		
Au1–Pt1–P2	123.9(1)		
(b)			
Pt2–Pt1–Au1	58.7(1)	S1–Pt2–P4	169.1(1)
Pt2–Pt1–S1	46.0(1)	S2–Pt2–P4	86.8(1)
Au1–Pt1–S1	45.0(1)	P3–Pt2–P4	98.5(1)
Pt2–Pt1–S2	45.7(1)	Pt1–Au1–Pt2	60.1(1)
Au1–Pt1–S2	60.3(1)	Pt1–Au1–S1	45.9(1)
S1–Pt1–S2	82.4(1)	Pt2–Au1–S1	46.8(1)
Pt2–Pt1–P1	130.5(1)	Pt1–Au1–S2	43.1(1)
Au1–Pt1–P1	128.0(1)	Pt2–Au1–S2	44.3(1)
S1–Pt1–P1	172.6(1)	S1–Au1–S2	70.5(1)
S2–Pt1–P1	91.4(1)	Pt1–Au1–P5	140.2(1)
Pt2–Pt1–P2	123.1(1)	Pt2–Au1–P5	142.1(1)
Au1–Pt1–P2	114.4(1)	S1–Au1–P5	168.6(1)
S1–Pt1–P2	87.2(1)	S2–Au1–P5	120.8(1)
S2–Pt1–P2	168.7(1)	Pt1–S1–Pt2	87.6(1)
P1–Pt1–P2	99.3(1)	Pt1–S1–Au1	89.1(1)
Pt1–Pt2–Au1	61.2(1)	Pt2–S1–Au1	86.7(1)
Pt1–Pt2–S1	46.4(1)	Pt1–S2–Pt2	89.0(1)
Au1–Pt2–S1	46.4(1)	Pt1–S2–Au1	76.6(1)
Pt1–Pt2–S2	45.3(1)	Pt2–S2–Au1	74.0(1)
Au1–Pt2–S2	61.7(1)		
S1–Pt2–S2	82.4(1)		
Pt1–Pt2–P3	130.8(1)		
Au1–Pt2–P3	113.7(1)		
S1–Pt2–P3	92.4(1)		
S2–Pt2–P3	174.6(1)		
Pt1–Pt2–P4	123.5(1)		
Au1–Pt2–P4	128.1(1)		

with a planar $\text{P}_2\text{PtS}_2\text{PtP}_2$ frame. The Pt atoms are 0.015 Å out of the least-squares plane through the 4 P and the 2S atoms, one Pt below and the other above that plane. Au is linearly coordinated (S–Au–Cl is 174.2°). The angle Au–S–Pt is 84.0° and Au–S–Pt¹ is 87.7° , the lowest angle of 84.0° corresponds with the Pt atom that comes up from the P_4S_2 -plane in the direction of the Au atom, the Au–Pt distance is 3.111 Å as compared with 3.28 Å for the Au–Pt¹ distance. This interesting detail in the molecular structure indicates a weak Pt–Au bonding interaction (Fig. 2). The bis-S-alkylated compounds $\text{Pt}_2(\text{PProp}_3)_4(\mu\text{-SEt})_2^{2+}$ [20] and $\text{Pt}_2(\text{PPh}_3)_2(\text{NO}_2)_2(\mu\text{-SMe})_2$ [18] both have a hinged square-planar geometry with hinge angles of 130° and 140° respectively. The Pt–S–C angles are in the range $110\text{--}140^\circ$, bending the alkyl groups away from the hinge. In the Pt–Au compound described here the bond angles on the S atoms are close to 90° . MO calculations [21] have shown that the energy involved in the hinging of coordination squares is relatively small and that subtle electronic and crystal packing effects determine the actual hinge angle.

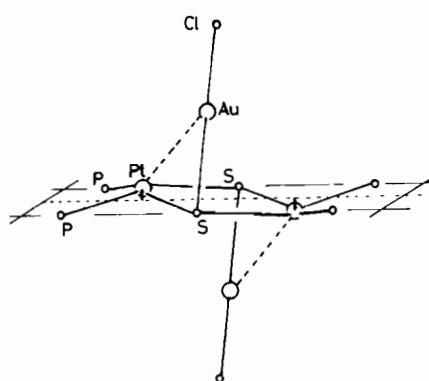


Fig. 2. The Pt–Au interactions indicated in a schematic figure of the molecular structure of $\text{Pt}_2(\text{PPh}_3)_4(\mu\text{-SAuCl})_2$.

When a suspension of $\text{Pt}_2(\mu\text{-S})_2(\text{PPh}_3)_4$ in THF is treated with 1 equivalent of $\text{AuPPh}_3\text{NO}_3$, $\text{Pt}_2(\text{PPh}_3)_4(\mu\text{-S})(\mu\text{-SAuPPh}_3)\text{NO}_3 \cdot 0.5\text{H}_2\text{O}$ is obtained as yellow crystals. Conductivity measurements in DMSO ($\Lambda_0 = 49.5 \text{ ohm}^{-1} \text{ cm}^2 \text{ mol}^{-1}$ at 25°C) and the infrared spectrum (free nitrate at 1360 cm^{-1}) are in agreement with the results of a single-crystal X-ray analysis. This shows $\text{Pt}_2(\text{PPh}_3)_4(\mu\text{-S})(\mu\text{-SAuPPh}_3)^+$ to have a hinged square-planar geometry with the hinge angle, that is the dihedral angle between the local coordination planes, of 135° . The Au–S distances 2.345 \AA and 2.959 \AA indicate that Au is coordinated to only one of the S-atoms. In these respects it resembles the methylated $\text{Pt}_2(\text{PPh}_3)_4(\mu\text{-S})(\mu\text{-SMe})^+$, which has a hinge angle of 138° [9]. In the Pd and Hg compounds both S atoms are coordinated, making $\text{Pt}_2(\text{PPh}_3)_4\text{S}_2$ a bidentate ligand [6]. The rather long Pt–Pt (3.279 \AA) and Pt–Au (3.314 and 3.231 \AA) distances give no evidence for metal–metal bonding. The gold atom is linear coordinated (S–Au–P angle is 168.6°). The Pt₁–S–Pt₂ angle is 87.6° , quite near to that in the forementioned methylated compound (88.9°). That methyl group is bended away from the hinge; Pt–S–C angles being 104.0° and 100.2° [6]. However, the S–Au vector is nearly perpendicular to the Pt–S–Pt plane, the Pt–S–Au angles are 86.7° and 89.1° .

$\text{Pt}_2(\text{PPh}_3)_4(\mu\text{-SAuPPh}_3)_2(\text{NO}_3)_2$ is formed when a suspension of $\text{Pt}_2(\mu\text{-S})_2(\text{PPh}_3)_4$ in THF is treated with 2 equivalents of $\text{AuPPh}_3\text{NO}_3$. The composition was established by analyses, conductivity measurements ($\Lambda = 59.2 \text{ ohm}^{-1} \text{ cm}^2 \text{ mol}^{-1}$ in DMSO, 25°C) which agrees with a 1:2 electrolyte and the molar weight determination. We suggest that this complex is built up in the same way as $\text{Pt}_2(\text{PPh}_3)_4(\mu\text{-SAuCl})_2$ with a planar $\text{P}_2\text{PtS}_2\text{PtP}_2$ frame and a linear coordinated gold atom on each side of that plane. Comparing the chemical shifts of the ^{31}P [^1H] NMR spectra of the three complexes: $\text{Pt}_2(\text{PPh}_3)_4(\mu\text{-S})(\mu\text{-SAuPPh}_3)$ IV: 17.95 ppm (P,PtPPh₃), 29.22 ppm (P,AuPPh₃); $\text{Pt}_2(\text{PPh}_3)_4(\mu\text{-SAuCl})_2$: 18.88 ppm (P,PtPPh₃); $\text{Pt}_2(\text{PPh}_3)_4(\mu\text{-SAuPPh}_3)_2(\text{NO}_3)_2$ III: 18.80 ppm (P, PtPPh₃), 32.90 ppm (P,AuPPh₃) (all shifts downfield relative to TMP in CH_2Cl_2), the suggestion of the structure of $\text{Pt}_2(\text{PPh}_3)_4(\mu\text{-SAuPPh}_3)_2(\text{NO}_3)_2$ is underlined.

In the reaction of one equivalent or an excess of AuPPh_3Cl with $\text{Pt}_2(\mu\text{-S})_2(\text{PPh}_3)_4$ only $\text{Pt}_2(\text{PPh}_3)_4(\mu\text{-S})(\mu\text{-SAuPPh}_3)^+$ is formed, while the reaction of $\text{Pt}_2(\text{PPh}_3)_4(\mu\text{-SAuPPh}_3)_2(\text{NO}_3)_2$ with Cl^- ions yields $\text{Pt}_2(\text{PPh}_3)_4(\mu\text{-S})(\mu\text{-SAuPPh}_3)^+$ and AuPPh_3Cl . Obviously Cl^- is successful in competing with $\text{Pt}_2(\text{PPh}_3)_4(\mu\text{-S})(\mu\text{-SAuPPh}_3)^+$ for AuPPh_3 while NO_3^- is not.

Acknowledgements

Acknowledgment is made to Professor Dr. Ir. J. J. Steggerda for his continuous interest. These investigations were supported in part by the Netherlands Foundation for Chemical Research (SON), with financial aid from the Netherlands Organization of Pure Research (ZWO).

References

- 1 D. A. Roberts and G. L. Geoffroy, in G. Wilkinson, F. G. A. Stone and E. W. Abel (eds.), 'Comprehensive Organometallic Chemistry', Pergamon, Oxford, 1982, Chap. 40.
- 2 P. Braunstein and J. Rose, *Gold. Bull.*, 18, 17 (1985).
- 3 J. J. Steggerda, J. J. Bour and J. W. A. van der Velden, *Recl. Trav. Chim. Pays-Bas*, 101, 164 (1982).
- 4 J. Evans and Jingxing Gao, *J. Chem. Soc., Chem. Commun.*, 39 (1985).
- 5 D. Seyferth, R. S. Henderson and Li-Cheng Song, *Organometallics*, 1, 125 (1982).
- 6 C. E. Briant, A. T. S. Hor, N. D. Howells and D. M. P. Mingos, *J. Chem. Soc., Chem. Commun.*, 1118 (1983).
- 7 R. Ugo, G. La Monica, S. Cenini, A. Segre and F. Conti, *J. Chem. Soc. A*, 522 (1971).
- 8 F. A. Vollenbroek, P. C. P. Bouten, J. M. Trooster, J. P. van den Berg and J. J. Bour, *Inorg. Chem.*, 17, 1345 (1979).
- 9 M. S. Lehman and F. K. Larsen, *Acta Crystallogr., Sect. A*, 30, 580 (1974).
- 10 D. F. Grant and E. J. Gabe, *J. Appl. Crystallogr.*, 11, 114 (1978).
- 11 A. C. T. North, D. C. Philips and F. S. Mathews, *Acta Crystallogr., Sect. A*, 24, 351 (1968).
- 12 G. M. Sheldrick, 'SHELX84', a program for crystal structure determination, Anorg. Chem. Inst. der Univ. Göttingen, F.R.G., 1984.
- 13 P. T. Beurskens, W. P. Bosman, H. M. Doesburg, Th. van den Hark, P. A. J. Prick, J. H. Noordik, G. Beurskens, R. O. Gould and V. Parthasarathi, in R. Srinivasan and R. H. Sarma (eds.), 'Conformation in Biology', Adenine, New York, 1982, p. 389.
- 14 G. M. Sheldrick, 'SHELX', a program for crystal structure determination, University Chemical Laboratory, Cambridge, U.K., 1976.
- 15 International Tables for X-ray Crystallography, Vol. IV, Kynoch Press, Birmingham, 1974.
- 16 N. Walker and D. Stuart, *Acta Crystallogr., Sect. A*, 39, 158 (1983).
- 17 W. D. Motherwell, 'PLUTO', a program for plotting molecular and crystal structures. University Chemical Laboratory, Cambridge, U.K. 1976.
- 18 C. E. Briant, C. J. Gardner, A. T. S. Hor, N. D. Howells and D. M. P. Mingos, *J. Chem. Soc., Dalton Trans.*, 2645 (1984).
- 19 J. W. A. Van der Velden, P. T. Beurskens, J. J. Bour, W. P. Bosman, J. H. Noordik, M. Kolenbrander and J. A. K. M. Buskes, *Inorg. Chem.*, 23, 146 (1984).
- 20 M. C. Hall, J. A. J. Jarvis, B. T. Kilbourn and P. G. Owston, *J. Chem. Soc., Dalton Trans.*, 1544 (1972).
- 21 R. H. Summerville and R. Hoffmann, *J. Am. Chem. Soc.*, 98, 7240 (1976).